Int. J. Solids Structures Vol. 27, No. 1, pp. 15–28, 1991
Printed in Great Britain.

0020–7683/91 $3.00+.00

ON DELAMINATION BUCKLING AND GROWTH IN CIRCULAR AND ANNULAR ORTHOTROPIC PLATES

PER-LENNART LARSSON
Department of Solid Mechanics, Royal Institute of Technology, S-100 44 Stockholm, Sweden
S-100 44 Stockholm, Sweden

(*Received* 12 *April* 1989; *in revised form* 30 *October* 1989)

Abstract—Buckling loads are determined numerically for isotropic and circumferentially orthotropic plates with regard to the presence of concentric delaminations of different geometries. For various combinations of geometry and material parameters, energy release rates are computed in the post-buckling range and predictions are made about the initiation and stability of crack growth.

1. INTRODUCTION

A serious but not infrequent cause of failure in laminates is due to inter-layer cracks or delaminations. Such flaws may be present already at fabrication or they may develop at quasi-static loading, in particular at free boundaries, and notoriously at impact. The resulting damage may lead to a severe degradation of stiffness and strength of a load-carrying member, and means to analyse the consequences are clearly desirable. In particular for compressed panels, the combined events of buckling and delamination growth may lead to catastrophic failure. Accordingly, with the increasing use of composites in design, such problems have received much attention in recent years, perhaps Chai *et al.* (1981) being the first investigators to study the problem in a systematic manner. Some of the major issues involved have been recently discussed in a survey by Storåkers (1989).

The present study is concerned with combined buckling and delamination growth in a radially compressed plate with and without a central hole. The material properties considered are axially orthotropic though homogeneous. Typically the analysis of the issues involved includes several steps; first the loading required to initiate buckling must be determined and an analysis of the ensuing post-buckling behaviour performed. Then criteria for initiation and continuation of growth of inter-layer cracks have to be applied and the effects as regards progressing delamination have to be predicted. The buckling analysis may be carried out in a traditional way although non-trivial technical issues may emerge for instance due to contact problems, in the post-buckling range. As regards initiation of crack growth and propagation, linear fracture mechanics is usually relied upon and such events are mostly assumed to occur at a constant value of the energy release rate. This issue is not without ambiguity though as it is fairly well established that inter-layer shearing modes are generally more resistant to growth. To take such aspects into account, a recent method proposed by Suo and Hutchinson (1988) and Suo (1988) for decomposition of crack growth modes in beams may be generalized and incorporated in the present problem without any fundamental difficulties. The more simple criterion involving the total energy release rate is, however, adopted presently.

Axisymmetric problems of the nature just outlined received some attention earlier as analyses based on first-order post-buckling theory have been carried out e.g. by Kachanov (1976), Bottega and Maewal (1983) and Evans and Hutchinson (1984). As emphasized by Yin (1985) however, in general, a fully nonlinear analysis is needed. The load required for initiation of buckling of an isotropic delaminated circular plate has been determined by Yin and Fei (1984) for various geometries and in particular for a thin delamination. Yin and Fei (1988) have also analyzed post-buckling and crack growth. Although much has been learnt about the phenomena involved, the situations dealt with have been restricted by special assumptions and particular geometries. The present contribution aims at greater

generality, by solving a set of fully nonlinear equations for buckling and delamination of a compressed plate and, in particular, including the effects of a central hole and anisotropy.

2. FIELD EQUATIONS

In von Karman kinematics for plates, the total strains are composed of a stretching term and a bending term such that

$$\varepsilon_r = \frac{du}{dr} + \frac{1}{2}\left(\frac{dw}{dr}\right)^2 - z\frac{d^2w}{dr^2}$$

$$\varepsilon_\theta = \frac{u}{r} - \frac{z}{r}\frac{dw}{dr} \tag{1}$$

in obvious notation when axisymmetry prevails.

The materials to be considered are assumed linear elastic though cylindrically orthotropic. Then the relations between middle surface strains and membrane forces N_r, N_θ may be written:

$$\frac{du}{dr} + \frac{1}{2}\left(\frac{dw}{dr}\right)^2 = \frac{1}{E_r t}(N_r - \nu_{r\theta}N_\theta)$$

$$\frac{u}{r} = \frac{1}{E_\theta t}(N_\theta - \nu_{\theta r}N_r) \tag{2}$$

where t is the plate thickness and the moduli E_r, E_θ and contraction ratio $\nu_{r\theta}$, $\nu_{\theta r}$ are related through $\nu_{r\theta}E_\theta = \nu_{\theta r}E_r$ by reciprocity.

Introducing the notation $k^2 = E_\theta/E_r$, $D_r = E_r t^3/[12(1-\nu_{r\theta}\nu_{\theta r})]$ the relations between curvatures and bending moments M_r, M_θ reduce to:

$$\frac{d^2w}{dr^2} = -\frac{1}{D_r}\frac{(M_r - \nu_{r\theta}M_\theta)}{(1-\nu_{r\theta}\nu_{\theta r})}$$

$$\frac{1}{r}\frac{dw}{dr} = -\frac{1}{k^2 D_r}\frac{(M_\theta - \nu_{\theta r}M_r)}{(1-\nu_{r\theta}\nu_{\theta r})}. \tag{3}$$

The single non-trivial in-plane equilibrium equation reads in case of axisymmetry

$$\frac{d}{dr}(rN_r) - N_\theta = 0 \tag{4}$$

expressed in cylindrical coordinates while the equation for transverse equilibrium reduces to

$$\frac{d}{dr}\left(\frac{d}{dr}(rM_r) - M_\theta\right) + \frac{d}{dr}\left(rN_r\frac{dw}{dr}\right) = -pr. \tag{5}$$

With no transverse loading present, either distributed, $p(r)$, or at the boundary, eqn (5) may be integrated once to read:

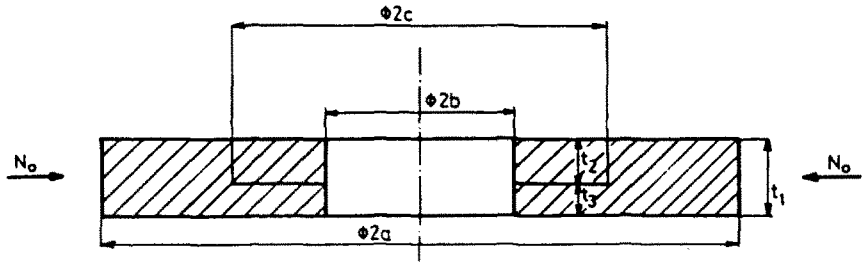

Fig. 1. Plate and delamination geometry.

$$\frac{\mathrm{d}}{\mathrm{d}r}(rM_r) - M_\theta = -rN_r\frac{\mathrm{d}w}{\mathrm{d}r}. \tag{6}$$

In Fig. 1 a circular plate is depicted containing a central hole of radius b and a circular delamination of radius c. The first task is to determine when this assembly, presently modelled as composed of three annular plates, buckles under an external compressive load N_0. To this end the field equations laid down above may be applied to each plate separately, supplemented with continuity conditions and boundary conditions. As regards the latter, the vanishing of any transverse shear force by (6) implies that the boundary conditions for a free edge and hinged edge reduces to

$$M_r = 0 \tag{7}$$

as a rigid-body transverse displacement is available. For a clamped edge the boundary condition is

$$\frac{\mathrm{d}w}{\mathrm{d}r} = 0. \tag{8}$$

For annular plates the hole boundary was in all cases assumed to be free, as was thought to be of most interest from a practical point of view.

At the outer boundary of the plate, $r = a$, the radial membrane force is

$$N_r = -N_0, \tag{9}$$

while at the hole, $r = b$,

$$N_r = 0. \tag{10}$$

It then remains to establish equations of compatibility and continuity of dynamic variables at the delamination front, $r = c$.

In Fig. 2 are shown details of the deformed geometry of the three plates, 1, 2, 3, at the delamination boundary. As regards kinematics, continuity of slope requires that

$$\frac{\mathrm{d}w_1}{\mathrm{d}r} = \frac{\mathrm{d}w_2}{\mathrm{d}r} = \frac{\mathrm{d}w_3}{\mathrm{d}r} \tag{11}$$

while continuity of radial displacements requires that

$$u_2 - u_1 = -\frac{t_3}{2}\frac{\mathrm{d}w_1}{\mathrm{d}r} \tag{12}$$

and

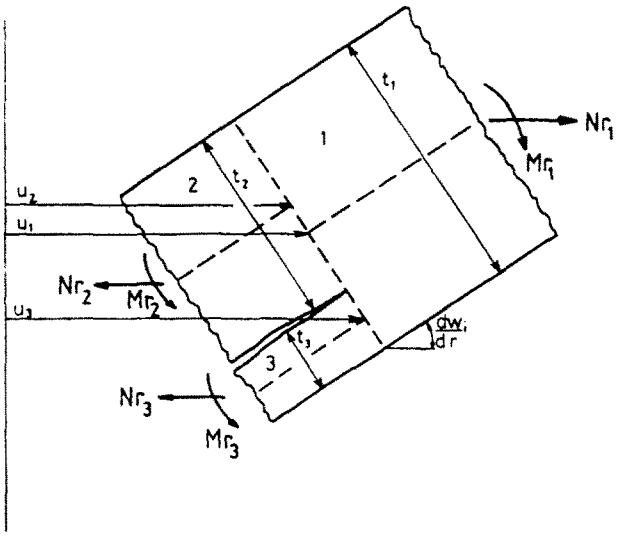

Fig. 2. Load resultants and displacements at the delamination front.

$$u_2 - u_3 = -\frac{t_1}{2}\frac{\mathrm{d}w_1}{\mathrm{d}r}. \tag{13}$$

Continuity of membrane forces and bending moments requires that

$$N_{r_1} = N_{r_2} + N_{r_3} \tag{14}$$

and

$$M_{r_1} = M_{r_2} + M_{r_3} + \tfrac{1}{2}(N_{r_2}t_3 - N_{r_3}t_2), \tag{15}$$

respectively.

This completes the setting of the boundary value problem, though for technical reasons at this instant it proves useful to introduce dimensionless variables according to

$$\rho = \frac{r}{a}$$

$$\phi_i = \frac{1}{\rho}\frac{\mathrm{d}}{\mathrm{d}\rho}\left(\frac{w_i}{t_i}\right)$$

$$P_i = \frac{N_{r_i}a^2}{D_{r_i}}, \tag{16}$$

$i = 1, 2, 3$, for the individual plates.

It is then a routine matter to combine the kinematical relations (1) and the constitutive eqns (2), (3) in order to write the equilibrium eqns (4) and (6) in dimensionless form. The result is

$$P_i'' + 3P_i'/\rho + (1-k^2)P_i/\rho^2 = -6k^2(1 - \nu_{r\theta}\nu_{\theta r})\phi_i^2 \tag{17}$$

and

$$\phi_i'' + 3\phi_i'/\rho + (1-k^2)\phi_i/\rho^2 = P_i\phi_i, \tag{18}$$

respectively, where a prime denotes differentiation with respect to ρ. The present formulation was first given by Bodner (1954) for an isotropic case.

The dimensionless variables may finally be introduced into the boundary conditions and the compatibility and continuity conditions at the delamination front, eqns (11)–(15), but the resulting explicit expressions are suppressed for brevity.

3. SOLUTION OF THE BUCKLING PROBLEM

The first step when performing the buckling analysis is to derive the pre-buckling membrane stress field by aid of eqn (17) with the right-hand side suppressed. Enforcing the boundary conditions (9) and (10) the solution is

$$P_i = -\frac{a^2}{D_{r_i}}\frac{t_i}{t_1}\frac{N_0}{(1-\rho_b^{2k})}\rho^{k-1}\left[1-\left(\frac{\rho_b}{\rho}\right)^{2k}\right] \tag{19}$$

for the individual plates.

In the case of a full plate, $\rho_b = 0$, eqn (18) with (19) inserted admits an analytical solution for the buckling mode expressible by aid of standard Bessel functions as

$$\phi_i = \frac{A_i}{\rho}\frac{J_{2k}}{k+1}\left(\frac{2\lambda_i}{k+1}\rho^{k+1/2}\right) + \frac{B_i}{\rho}\frac{Y_{2k}}{k+1}\left(\frac{2\lambda_i}{k+1}\rho^{k+1/2}\right) \tag{20}$$

where A_i, B_i are arbitrary amplitudes and

$$\lambda_i^2 = \frac{N_0 a^2}{D_{r_i}}\frac{t_i}{t_1}.$$

It should be emphasized, however, that here and in the following, only axisymmetric buckling modes are considered, as it is believed that in general for the cases to be dealt with, they are associated with the lowest buckling load.

In order to completely set the eigenvalue problem, the confrontation of (20) with relevant boundary conditions is quite straightforward and so also is the case for the continuity condition (14). Enforcement of the remaining conditions (12), (13) and (15) requires some reflection, however, as regards retention of terms of relevant order.

To this end the variables present in (12) and (13) were expressed by using series expansion in the post-buckling range. Then by using the pre-buckling solution (19), the remaining condition (15) reduces to

$$M_{r_1} = M_{r_2} + M_{r_3} - \frac{E_r t_1 t_2 t_3 (k^2 - v_{\theta r}^2)(c^{2k} - b^{2k})}{4(1 - v_{r\theta}v_{\theta r})[(k - v_{\theta r})c^{2k} + (k + v_{\theta r})b^{2k}]}\frac{1}{c}\frac{dw_1}{dr}, \tag{21}$$

where the bending moments may be expressed by using the deflection slope through the constitutive eqns (3).

For the case of a full plate, determination of the critical value of $N_0(\lambda_1^2)$ is now quite straightforward by introducing (20) into the external boundary condition (7) or alternatively, (8) together with the continuity conditions (11) and (21) expressed in the dimensionless variables ϕ_i, according to (16). The result is a system of homogeneous equations generating the required eigenvalues.

For a plate with a central hole, $\rho_b \neq 0$, however, the situation becomes somewhat more involved. This derives from the fact that no analytical solutions may be found for the buckling modes ϕ_i. This is no major obstacle though as the governing differential eqn (18) may be readily solved by using a standard computer procedure based on Merson's form of the Runge–Kutta method for simultaneous ordinary first-order equations. With this tool

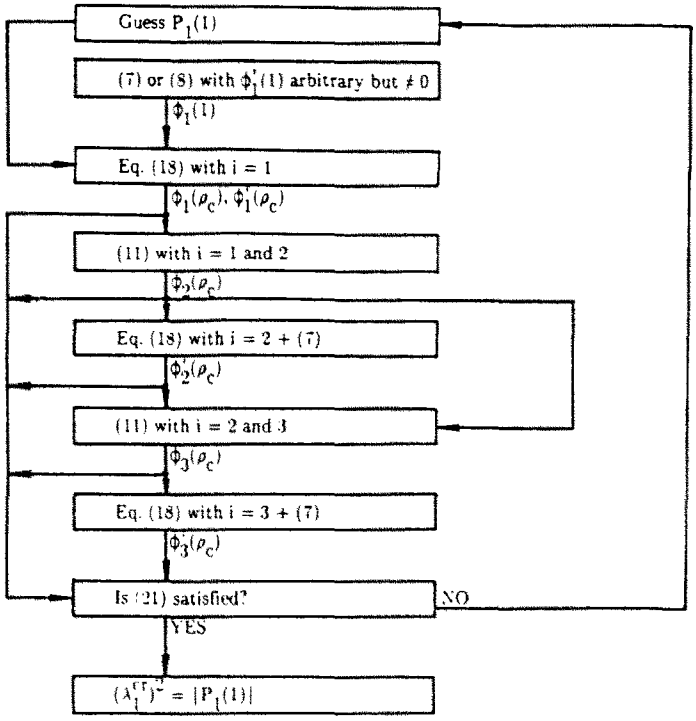

Fig. 3. Algorithm scheme for solution of the eigenvalue problem.

available the required eigenvalue may be found by a "shooting method" based on an algorithm details of which are depicted in Fig. 3.

In the post-buckling range the governing differential eqns (17) and (18) have to be solved in full and simultaneously. Also for this case, however, the computer procedure just outlined may be used to advantage to solve four coupled nonlinear first-order equations utilizing Newton iteration. Technically the problem to determine the post-buckling behaviour of the three-plate assembly with due account of continuity is somewhat complicated and a suitable algorithm has to be designed. Again it was found advantageous to use a "shooting method" and the details of the final procedure adopted is depicted in Fig. 4 which is believed to be self-explanatory.

4. THE ENERGY RELEASE RATE AT DELAMINATION GROWTH

As has already been forecast, the criterion adopted for initiation and continuation of delamination growth is that the energy release per unit area of growth will attain a critical and constant value. When crack growth is self-similar or when the crack contour may be reproduced by a discrete set of parameters there is no fundamental difficulty in determining the rate of change of potential energy of the system. For a problem similar to the present this method has been adopted e.g. by Evans and Hutchinson (1984) for the initial post-buckling range. In an alternative approach for a circular crack Yin (1985) and Yin and Fei (1988) have used the local value of a small strain version of the M-integral.

Local values of the energy release rate with due account of nonlinear kinematics in a general situation have recently been derived by Storåkers and Andersson (1988) starting from von Karman plate theory and first principles. Thus these writers found that the energy released at crack advance $\delta a(x_\alpha)$ at a crack contour Γ_c having the local normal n_α, could be expressed as

$$-\delta U = \int \| P_{\alpha\beta} \| n_\alpha n_\beta \delta a \, \mathrm{d}\Gamma_c \tag{22}$$

where $P_{\alpha\beta}$ is a plate analogue of Eshelby's energy momentum tensor and $\| \quad \|$ denotes its jump determined from the individual plate members intersecting at the crack front.

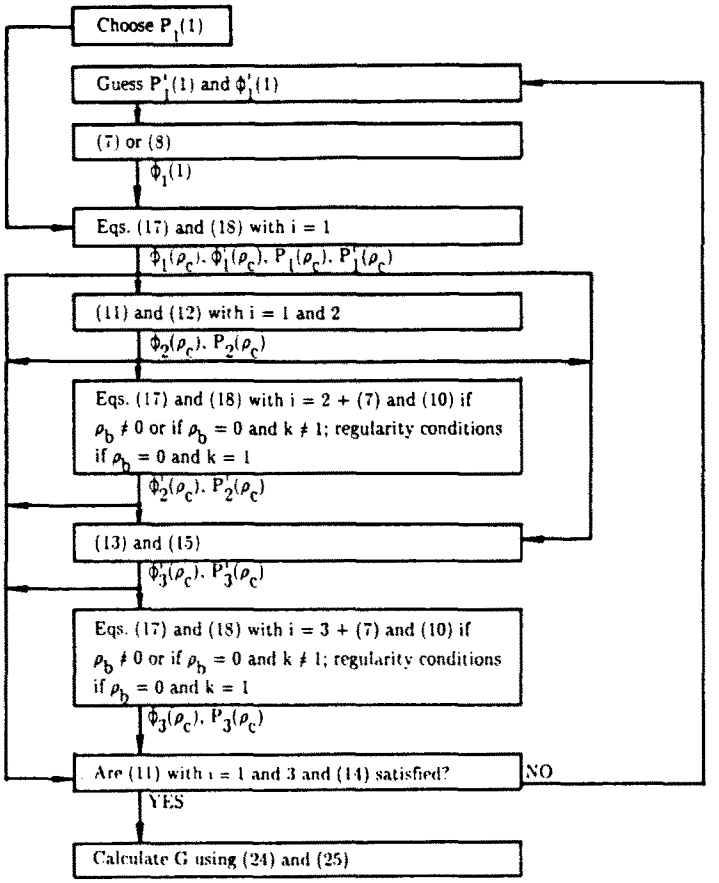

Fig. 4. Algorithm scheme for solution of the post-buckling problem.

Explicitly $P_{\alpha\beta}$ reads

$$P_{\alpha\beta} = W\delta_{\alpha\beta} - N_{\alpha\gamma}u_{\gamma,\beta} + M_{\alpha\gamma}u_{3,\gamma\beta} - Q_\alpha u_{3,\beta}, \tag{23}$$

where W denotes the plate strain energy density and the jump of the last term, involving shear forces, vanishes due to continuity.

It is now convenient to use the axisymmetric reduced form of (22) and determine the released energy per unit area as

$$G = P_1 - P_2 - P_3 \tag{24}$$

in obvious notation.

By aid of the adopted constitutive equation, derivation of the P_i values for the individual plates expressed in radial and transversal displacements is quite straightforward. The result is

$$P_i = -\frac{E_r t_i}{2(1-\nu_{r\theta}\nu_{\theta r})}\left\{\left(\frac{\mathrm{d}u_i}{\mathrm{d}r}\right)^2 - k^2\left(\frac{u_i}{r}\right)^2 - \frac{1}{4}\left(\frac{\mathrm{d}w_i}{\mathrm{d}r}\right)^2 - \nu_{\theta r}\frac{u_i}{r}\left(\frac{\mathrm{d}w_i}{\mathrm{d}r}\right)^2 + \frac{t_i^2}{12}\left[\left(\frac{\mathrm{d}^2 w_i}{\mathrm{d}r^2}\right)^2 - \frac{k^2}{r^2}\left(\frac{\mathrm{d}w_i}{\mathrm{d}r}\right)^2\right]\right\}. \tag{25}$$

Once the post-buckling solution is known it is then a routine matter to determine the

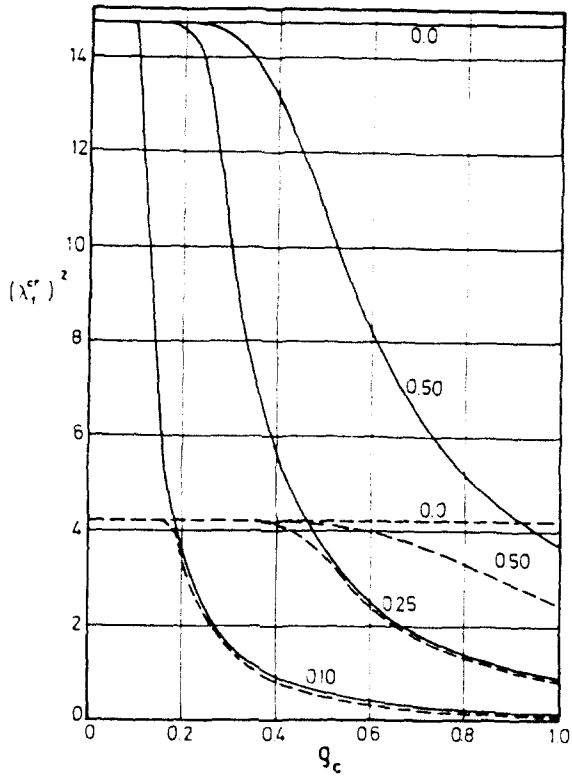

Fig. 5. Buckling load, $(\lambda_1^{cr})^2 = -N_0^{cr}a^2/D_{r_1}$, for a full isotropic plate as a function of crack radius, $\rho_c = c/a$, for different values of delamination thickness, $\tau = t_3/t_1$; (——) clamped boundary, (– – –) simply supported boundary.

energy release rate by use of (24) and (25). When presenting explicit results it proves suitable though to introduce a dimensionless measure defined by

$$\bar{G} = \frac{(1-\nu_{r\theta}\nu_{\theta r})a^4}{E_r t_1^5} G. \tag{26}$$

In their analysis Storåkers and Andersson (1988) also discussed ways of improving the accuracy by basing determination of the energy release rate on dynamic variables and also using balance equations for the energy momentum tensor. The post-buckling solution is, however, believed to generate high accuracy and (25) will be strictly adhered to.

5. RESULTS AND DISCUSSION

The first issue of interest concerns the influence of delamination geometry and constitutive properties on the buckling load. The results for a full isotropic plate are shown in Fig. 5 for three values of the delamination thickness. Here the value 0.3 has been chosen for Poisson's ratio and also in the sequel for ν_{0r}. It is evident that at smaller delamination radii, the behaviour is overall buckling at a load only slightly affected by the presence of a delamination. On the other hand, save for a mid-plane delamination, $\tau = 0.5$ ($\tau = t_3/t_1$) at larger radii buckling is local with respect to the thinnest delaminated layer and the critical load is virtually independent of the external boundary conditions. If the radius representing the wavelength of the deformed profile of an undamaged plate is denoted by ρ^* the transition point from overall to local buckling occurs at $\rho_c/\rho^* \cdot \tau = 2$ for both simply supported and clamped external boundary conditions. This finding essentially agrees with that of Yin and Fei (1984) in their analysis of the present eigenvalue problem. The general features are also very similar to those found by Simitses *et al.* (1985) for a corresponding rectilinear case. The results given in Fig. 5 indicate when a so-called thin film approximation is applicable

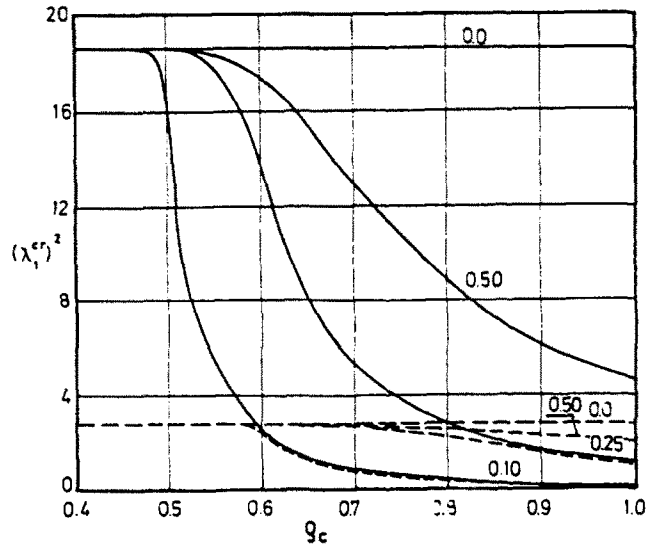

Fig. 6. Buckling load, $(\lambda_1^{cr})^2 = -N_0^{cr}a^2/D_{r_1}$, for an annular isotropic plate as a function of crack radius, $\rho_c = c/a$, for different values of delamination thickness, $\tau = t_3/t_1$, $\rho_b = 0.4$; (——) clamped outer boundary, (– – –) simply supported outer boundary.

to determine the initiation of buckling. In this approach transverse deflection is disregarded save for the thin delaminated part.

The results for a plate having a central hole with radius $\rho_b = 0.4$ are shown in Fig. 6. The sensitivity of the buckling load to the delamination size is of the same character showing a substantial decrease beyond a certain delamination radius although the transition value is now naturally increased. Essentially the same features were found to prevail for the case of orthotropy, $k > 1$, as regards the relation between buckling load and delamination size. The quantitative stiffening is, however, dependent on the buckling mode and this effect is depicted in Fig. 7 for the three different delamination thicknesses. As may be seen for small

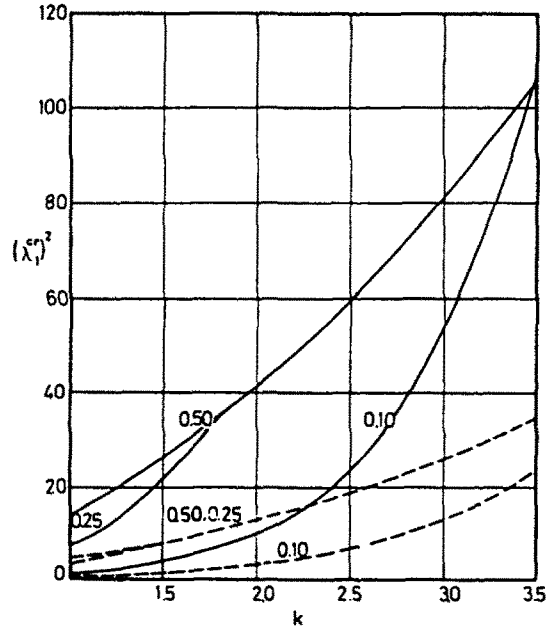

Fig. 7. Buckling load, $(\lambda_1^{cr})^2 = N_0^{cr}a^2/D_{r_1}$, for a full orthotropic plate as function of modulus ratio, $k^2 = E_\theta/E_r$, for different values of delamination thickness, $\tau = t_3/t_1$; (——) clamped boundary $\rho_c = 0.35$, (– – –) simply supported boundary $\rho_c = 0.5$.

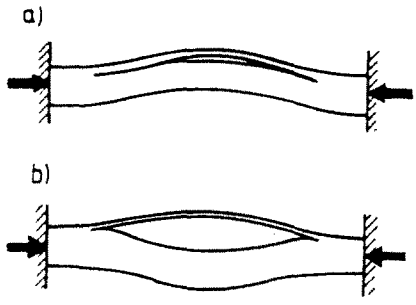

Fig. 8. Deflection modes in the post-buckling range.

values of k, thin film buckling, at $\tau = 0.1$, is less sensitive to k while at larger values the opposite is true.

In all cases dealt with the initial buckling mode was as depicted in Fig. 8a, that is every plate element deflected transversally in the same direction. In the post-buckling range, however, a snap-through into a mode according to Fig. 8b occurred shortly after buckling for $\tau = 0.1$ and 0.25.

As has become evident, especially thin delaminations may cause a dramatic reduction of the load required for initiation of buckling. This by no means implies that the load-carrying capacity is exhausted but that the compressive stiffness of the plate assembly undergoes only a slight decrease. No details will be dwelt upon as regards this phenomenon but suffice it to mention that in the case of $\tau = 0.1$, $\rho_c = 0.5$ and a full isotropic plate the stiffness was reduced by less than 3% at an external load being eight times the buckling load. Similarly for $\tau = 0.25$ the reduction was approximately 14% at three times the buckling load.

Instead the interest will now be focussed on the energy release rate at progressing delamination. The dimensionless energy release rate as a function of external loading in the post-buckling range is given for three values of the delamination radius in Fig. 9 for a thin delamination and in Fig. 10 for a moderately thin one. In both situations the energy release rate increases with the external loading and also for an increasing delamination radius. Thus within the Griffith philosophy unstable crack propagation is to be expected in par-

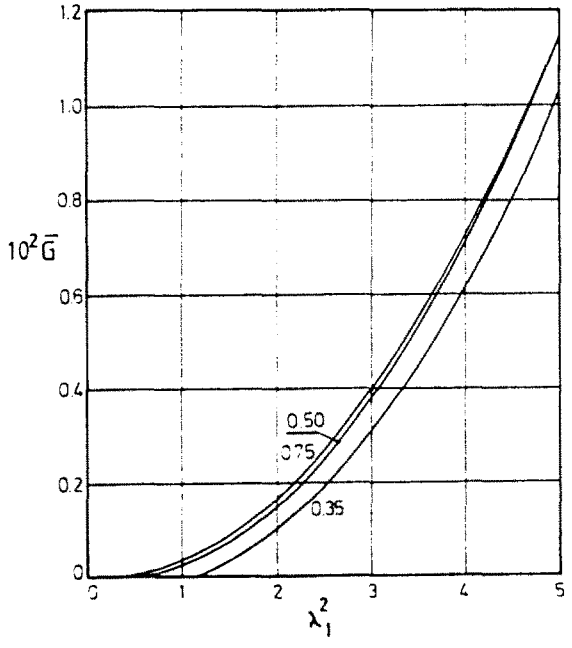

Fig. 9. Energy release rate, $\bar{G} = (1-\nu_{r\theta}\nu_{\theta r})a^4/E_r t_1^3\, G$, for a full isotropic plate as function of load, $\lambda_1^2 = N_0 a^2/D_{r_1}$, for different values of delamination radius, $\rho_c = c/a$, $\tau = 0.1$, clamped boundary.

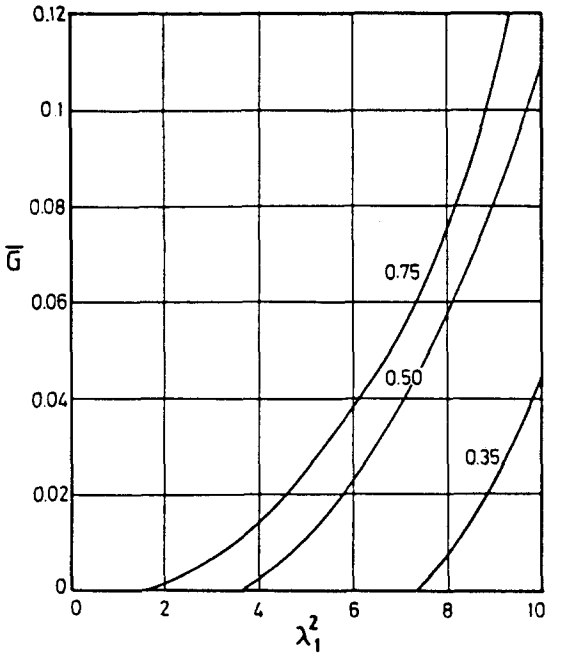

Fig. 10. Energy release rate, $\bar{G} = (1 - \nu_{r\theta}\nu_{\theta r})a^4/E_r t_1^3\, G$, for a full isotropic plate as function of load, $\lambda_1^2 = N_0 a^2/D_{r_1}$, for different values of delamination radius, $\rho_c = c/a$, $\tau = 0.25$, clamped boundary.

ticular for stubbier delaminations. Again the circumstances prevailing are similar to those of a rectilinear case as analysed by Yin *et al.* (1986). These writers predicted that for compressed wide columns, delamination buckling followed by growth is with few exceptions an unstable process.

In order to investigate associated load-deflection relations at eventual delamination growth, results are given in Fig. 11 for two values of the relative delamination thicknesses as in Figs 9 and 10. In both cases buckling was essentially local and in the thicker case, $\tau = 0.25$, the relative deflection was around 0.5 at twice the buckling load while the thinner one, $\tau = 0.1$, was essentially less so.

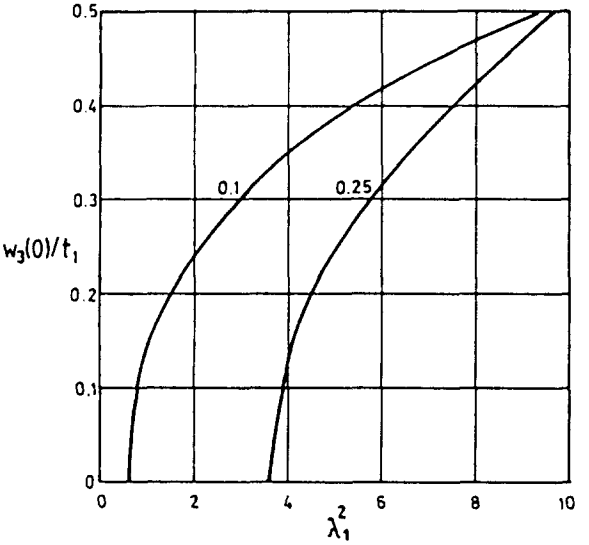

Fig. 11. Transversal displacement, $w_3(0)/t_1$, for a full isotropic plate as function of load, $\lambda_1^2 = N_0 a^2/D_{r_1}$, for different values of delamination thickness, $\tau = t_3/t_1$, $\rho_c = 0.5$, clamped boundary.

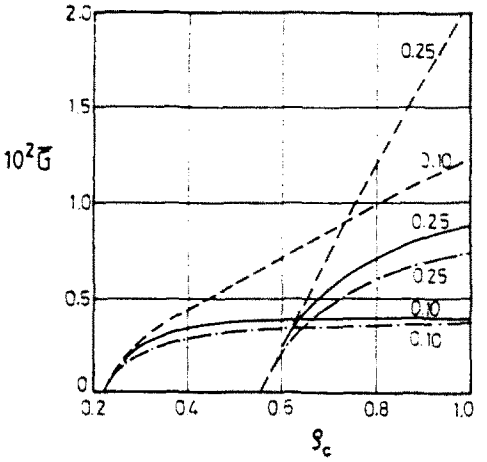

Fig. 12. Energy release rate, $\bar{G} = (1-\nu_{rz}\nu_{\theta z})a^4/E_r t_1^3\, G$, for a full isotropic plate as function of delamination radius, $\rho_c = c/a$, for different values of delamination thickness, $\tau = t_3/t_1$, $\lambda_1^2 = 3$; (——) clamped boundary, (– – –) simply supported boundary, (– · –) thin film approximation.

It is of particular interest to investigate the accuracy of the frequently employed thin film approximation in the present context. To this end a comparison of energy release rates is made in Fig. 12 where exact results and those of a thin film analysis are shown for a chosen load in the post-buckling range for different delamination radii. The agreement is quite satisfactory in the case of clamped plates even for a relative delamination thickness of 0.25 though the thin film results are slightly non-conservative from the view-point of crack propagation. In the case of simple support, however, it is only in the very initial stages of post-buckling that the thin film approximation may be applied to determine energy release rates with some confidence.

For a full isotropic plate Yin and Fei (1988) studied the case of a thin delamination, $\tau = 0.1$, approximately with the complete von Karman equations applied to the thin part of the plate assembly and linear equations to the remainder. Comparison was made with the results of these writers for $\rho_c = 0.25$ and the agreement found was excellent. Thus confidence was gained as regards the accuracy of the present number method and also as regards the relevance of the approximation made by Yin and Fei.

For annular plates the situation becomes somewhat more involved. Figure 13 shows that for a plate with a relative internal hole radius of 0.4 at a given load the energy release rate might attain a maximum for a particular delamination radius. Thus there exists a possibility that progressing delamination may be arrested. This being so for externally clamped plates, on the contrary a simple support crack will always be unstable in the sense discussed regardless if a central hole is present or not. Since circumstances prevailing in practice are, however, almost certain to be a combination of the two boundary conditions discussed, crack arrest is not likely to occur in such members.

The effect just discussed is, however, material dependent as illustrated in Fig. 14. Thus with the same plate and delamination geometry as for the isotropic case, when $k = 2$, crack growth is predicted to be unstable regardless of boundary conditions and eventually is so whether a central hole is present or not.

No results have been given in the post-buckling range for the case of a mid-plane delamination. This is due to the finding that almost immediately after buckling, crack closure occurred in the vicinity of the delamination boundary for values of τ close to or equal to 0.5. This proved to be the case for both full and annular plates at essentially global buckling. Contact problems of this kind may not be accommodated properly within the algorithm used, and the effect of this phenomenon will be dealt with elsewhere.

6. CONCLUDING REMARKS

The presence of delaminations might decrease the buckling load for full and annular plates drastically. It was found that, at least for moderately thin delaminations, the behav-

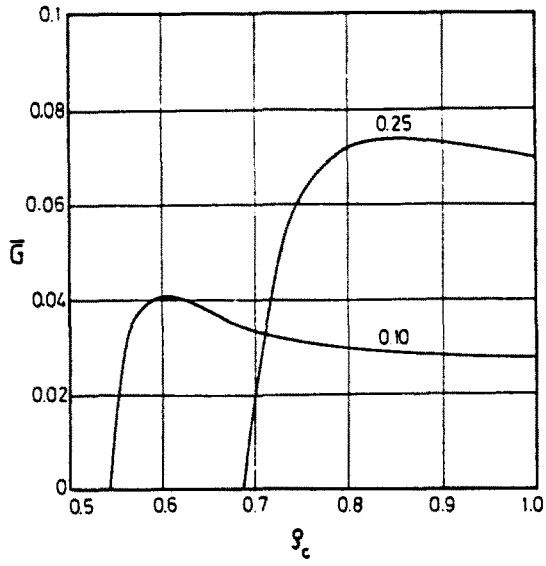

Fig. 13. Energy release rate, $\bar{G} = (1-\nu_{r\theta}\nu_{\theta r})a^4/E_r t_1^3\, G$, for an annular isotropic plate as function of delamination radius, $\rho_c = c/a$, for different values of delamination thickness, $\tau = t_3/t_1$, $\rho_h = 0.4$, $\lambda_1^2 = 6$, clamped outer boundary.

iour was one of either overall or local buckling with a rather narrow transition zone with respect to delamination size. Although the effect on post-buckling stiffness might not be severe, within the Griffith philosophy eventual delamination growth was in general predicted to be unstable at least for full isotropic plates. In order to arrive at conservative estimates an imperfection sensitivity analysis is then warranted. In the advanced post-buckling range, however, shear modes might dominate crack growth. Whether this feature might lead to crack arrest deserves a separate study, also as for annular plates, indications of crack arrest were found, though not in the presence of anisotropy.

A thin film approximation proved to be adequate in particular circumstances although it became apparent that the boundary conditions may play an important role for a member of finite size. In the case of very thick delaminations crack closure effects are to be expected.

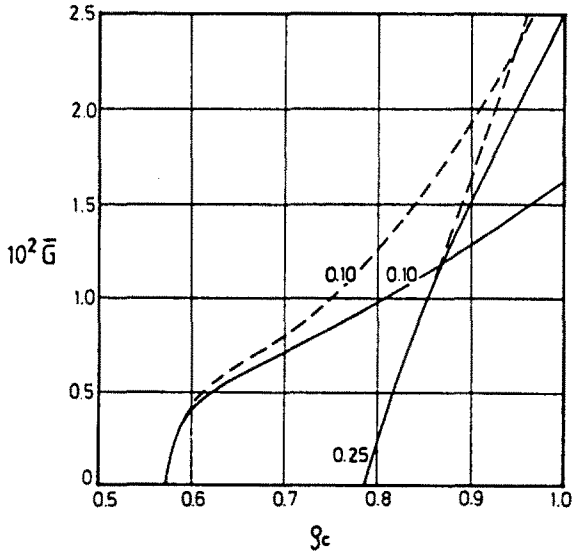

Fig. 14. Energy release rate, $\bar{G} = (1-\nu_{r\theta}\nu_{\theta r})a^4/E_r t_1^3\, G$, for an annular orthotropic plate as function of delamination radius, $\rho_c = c/a$, for different values of delamination thickness, $\tau = t_3/t_1$, $\rho_h = 0.4$, $k = 2$, $\lambda_1^2 = 6$; (——) clamped outer boundary, (– – –) simply supported outer boundary.

Acknowledgements—I would like to thank Professor Bertil Storåkers for his willingness to give helpful advice.

REFERENCES

Bodner, S. (1954). The post buckling behaviour of a clamped circular plate. *J. Appl. Math.* **12**, 397–401.

Bottega, W. J. and Maewal, A. (1983). Delamination buckling and growth in laminates. *J. Appl. Mech.* **50**, 184–189.

Chai, H., Babcock, C. D. and Knauss, W. G. (1981). One dimensional modelling of failure in laminated plates by delamination buckling. *Int. J. Solids Structures* **17**, 1069–1083.

Evans, A. G. and Hutchinson, J. W. (1984). On the mechanics of delamination and spalling in compressed films. *Int. J. Solids Structures* **20**, 455–466.

Kachanov, L. M. (1976). Separation failure of composite materials. *Polymer Mech.* **12**, 812–815.

Simitses, G. J., Sallam, S. and Yin, W. L. (1985). Effect of delamination of axially loaded homogeneous plates. *AIAA Jl* **23**, 1437–1444.

Storåkers, B. (1989). Nonlinear aspects of delamination in structural members. In *Proc. XVII Int. Congr. Theoretical and Applied Mechanics*. (Edited by P. Germain, M. Piau and D. Caillene), pp. 315–336. Elsevier, Amsterdam.

Storåkers, B. and Andersson, B. (1988). Nonlinear plate theory applied to delamination in composites. *J. Mech. Phys. Solids* **36**, 689–718.

Suo, Z. (1988). Delamination specimens for orthotropic materials. Harvard University Report MECH-135.

Suo, Z. and Hutchinson, J. W. (1988). Interface crack between two elastic layers. *Int. J. Fracture* (to appear).

Yin, W. L. (1985). Axisymmetric buckling and growth of a circular delamination in a compressed laminate. *Int. J. Solids Structures* **21**, 503–514.

Yin, W. L. and Fei, Z. (1984). Buckling load of a circular plate with a concentric delamination. *Mech. Res. Comm.* **11**, 337–344.

Yin, W. L. and Fei, Z. (1988). Delamination buckling and growth in a clamped circular plate. *AIAA Jl* **26**, 438–445.

Yin, W. L., Sallam, S. and Simitses, G. J. (1986). Ultimate axial load capacity of a delaminated plate. *AIAA Jl* **24**, 1–7.